# Is a $C_s$ Corrector Necessary for Lorentz Vector Field Tomography?

Charudatta Phatak, Marc De Graef
*Carnegie Mellon University, Pittsburgh*
*cd@cmu.edu*

Magnetic recording media based on patterned shapes are promising for applications in high density data storage. Optimizing the design of the patterned arrays requires characterization of the particle shapes and their relative locations, and the magnetostatic interactions between particles. To achieve this, one must determine the three dimensional (3D) magnetic induction in and around the nano magnets. We propose a method based on Vector Field Electron Tomography coupled with phase reconstructed Lorentz Microscopy to determine the 3D magnetic induction. This method can be broken down into two steps 1) Determination of the magnetic phase shift of the electron wave using phase reconstructed Lorentz microscopy and 2) Reconstruction (in 3D) of the magnetic induction in and around the magnetic particle using Vector Field Electron Tomography (VFET). First, we will discuss the theoretical development of VFET and then the importance of spherical aberration ($C_s$) correctors for Lorentz microscopy.

Lorentz Microscopy has been used mostly for qualitative magnetic characterization in Transmission Electron Microscopy (TEM). In the classical approach, a high energy electron beam in a TEM is deflected by the Lorentz force caused by the magnetic induction in and around the thin foil. The deflection angle is of the order of microradians and is given by:

$$\theta_L = \frac{e\lambda}{h} B_\perp t$$

This leads to two experimental modes of observation, Fresnel (out-of-focus imaging) and Foucault (dark field imaging). This approach adequately explains the commonly observed contrast features in both imaging modes. However, to formulate a quantitative understanding of Lorentz microscopy, especially Fresnel imaging, we have to use the quantum mechanical approach. According to this approach, an electron traveling through a thin foil with inner electrostatic potential V and magnetic vector potential A, experiences a phase shift given by:

$$\varphi = \varphi_e + \varphi_m = \sigma \int_L V(\mathbf{r})\mathrm{d}z - \frac{e}{h}\int_L \mathbf{A}(\mathbf{r})\cdot\mathrm{d}\mathbf{r}$$

where the integrals are taken along the electron trajectory [1]. The magnetic component of the phase shift can be rewritten as:

$$\varphi_m = \pi \frac{\Phi_m}{\Phi_0}$$

where $\Phi_0$ is the flux quantum. The magnetic phase shift is thus equal to the flux enclosed between the electron trajectory and a reference trajectory, in units of the flux quantum. The resulting electron exit wave function can be written as:

$$\psi(\mathbf{r}) = \sqrt{I(\mathbf{r}_\perp)}\mathrm{e}^{\mathrm{i}\varphi(\mathbf{r}_\perp)}\mathrm{e}^{\mathrm{i}\mathbf{k}\cdot\mathbf{r}}$$

Using this equation, Lorentz images can be simulated using an approach similar to standard High Resolution Electron Microscopy (HREM) image simulations.

Next, we must recover the magnetic phase shift from the Lorentz images. The total phase shift of the electron wave can be determined using either electron holography or by application of the Transport-of-Intensity (TIE) formalism. The latter formalism is based on the TIE equation, which can be written as:

$$\nabla\cdot(I(\mathbf{r},0)\nabla\phi) = -\frac{2\pi}{\lambda}\frac{\partial I(\mathbf{r},0)}{\partial z} \approx -\frac{2\pi}{\lambda}\frac{I(\mathbf{r},+\Delta f) - I(\mathbf{r},-\Delta f)}{2\Delta f}$$

where the 2D nabla operator works in the plane normal to the electron beam. The right hand side of the equation can be computed from the experimental Fresnel images, and the equation can be solved for the phase using a Fourier transform approach [2]. Once the total phase is obtained, the sample is then flipped by 180° and again the TIE formalism is applied to recover the phase. Due to the flip, the electrostatic phase shift remains the same whereas the magnetic phase shift changes sign. Thus by subtracting the phase of the flipped sample from that of the unflipped sample, the magnetic phase shift can be extracted.

Tomography is a method to reconstruct a 3D object from its 2D projections. While electron tomography has been used for a long time in the study of biological structures and molecules [3], vector field electron tomography is a lesser known technique that can be used to determine 3D magnetic induction. For a comprehensive study of vector field tomography we refer the reader to [4]. The phase shift of the electron wave, described in the previous section, can be expressed in terms of tomographic quantities. The electrostatic phase shift corresponds to a scalar x-ray transform and the magnetic phase shift is described by the vector x-ray transform. The magnetic phase shift can be rewritten as:

$$(\nu_{\hat{\omega}}\mathbf{A})(\xi) = \hat{\omega}\cdot\int_{-\infty}^{+\infty}\mathbf{A}(x,z)\mathrm{d}r$$

$$(\nu_{\hat{\omega}}\mathbf{A})(\xi) = \int_{-\infty}^{+\infty}[-\sin\theta A_x(\xi,\eta) + \cos\theta A_z(\xi,\eta)]\mathrm{d}r$$

where A is the magnetic vector potential of the particle and theta is the angle of tilt about the x axis. In Fourier space, this equation can be written as:

$$(\tilde{\nu}_\theta\mathbf{A})(\kappa) = -\sin\theta\tilde{A}_x(k_x,k_z) + \cos\theta\tilde{A}_z(k_x,k_z)$$

One of the components of magnetic induction B can be expressed as:

$$B_y(x,z) = (\nabla\times\mathbf{A})\cdot\hat{\mathbf{y}} = \frac{\partial A_x}{\partial z} - \frac{\partial A_z}{\partial x}$$

or, in Fourier Space, as:

$$\tilde{B}_y(k_x,k_z) = \mathrm{i}k_z\tilde{A}_x[k_x,k_z] - \mathrm{i}k_x\tilde{A}_z[k_x,k_z].$$

Comparing the two equations, we get:

$$\mathrm{i}\kappa(\tilde{\nu}_{\hat{\omega}}\mathbf{A})(\kappa) = -\tilde{B}_y(\kappa\cos\theta,\kappa\sin\theta)$$

This equation is the vector form of the Fourier Slice theorem. By taking an inverse Fourier Transform, the *y*-component of the magnetic induction can be recovered in real space. Similarly, by taking another tilt series around the *y*-axis, the *x*-component of the magnetic induction can be recovered. The third component can be

https://doi.org/10.1017/S1551929500061927 Published online by Cambridge University Press

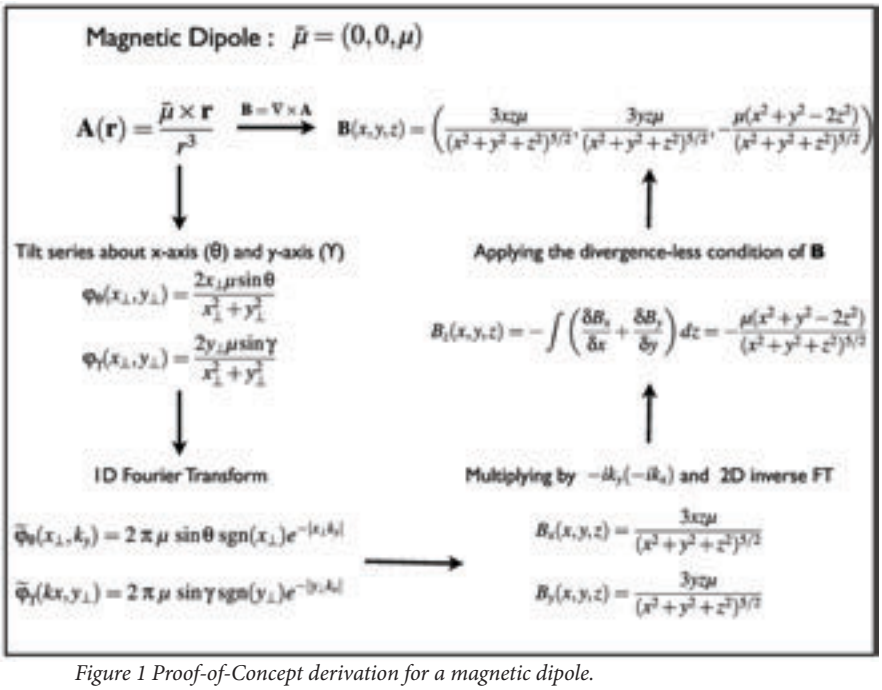


*Figure 1 Proof-of-Concept derivation for a magnetic dipole.*

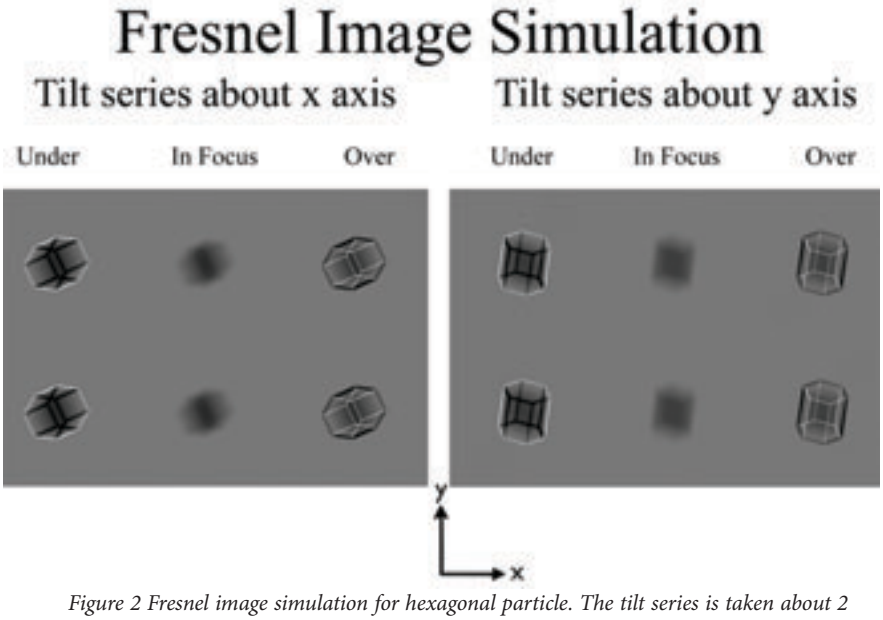


*Figure 2 Fresnel image simulation for hexagonal particle. The tilt series is taken about 2 orthogonal axes.*

obtained by using the divergenceless condition on ***B***. Thus, the complete 3D magnetic induction can be obtained in and around the magnetic particle. Figure 1 shows a proof of concept derivation of the complete VFET procedure for magnetic dipole. Since any 3D field can be considered as a superposition of dipole fields and since all the operations involved in VFET are linear, theoretically any 3D field can be reconstructed.

Since the method relies upon faithful reconstruction of the magnetic phase shift, we have studied the effect of the most important aberration, the spherical aberration, on the phase reconstruction and reconstructed 3D magnetic induction. Simulations were performed using a hexagonal prism with dimensions a = 20 nm and c = 40 nm. The saturation magnetic induction of the particle was taken to be 1 T, uniformly along the c-axis. The particle was oriented such that the c-axis was in the *x-y* plane. The theoretical phase shifts for the particle were computed using the shape amplitude formalism given in [5]. In the Lorentz transfer function, the spherical aberration was varied from 100 mm for a typical Lorentz lens to 0.05 mm for a corrected lens. Table 1 shows the microscope parameters for 3 different microscopes used for simulations; $q_c$ is the beam coherence and $D$ is the defocus spread. $Df$ is the defocus step size used for Fresnel imaging. Figure 2 shows the Fresnel image simulation for two tilt series.

Phase reconstruction was performed on these images followed by tomographic reconstruction. The tomographic reconstruction was performed using the filtered back projection method. Figure 3(a) shows the theoretical magnetic phase shift for the particle and (b)-(d) show the recovered phase shift for the 3 microscope settings. The bottom row of Table 1 shows the root-mean-square error (RMSE) of the reconstructed phase. It is clear that the phase recovery is the most accurate for the $C_s$ corrected microscope.

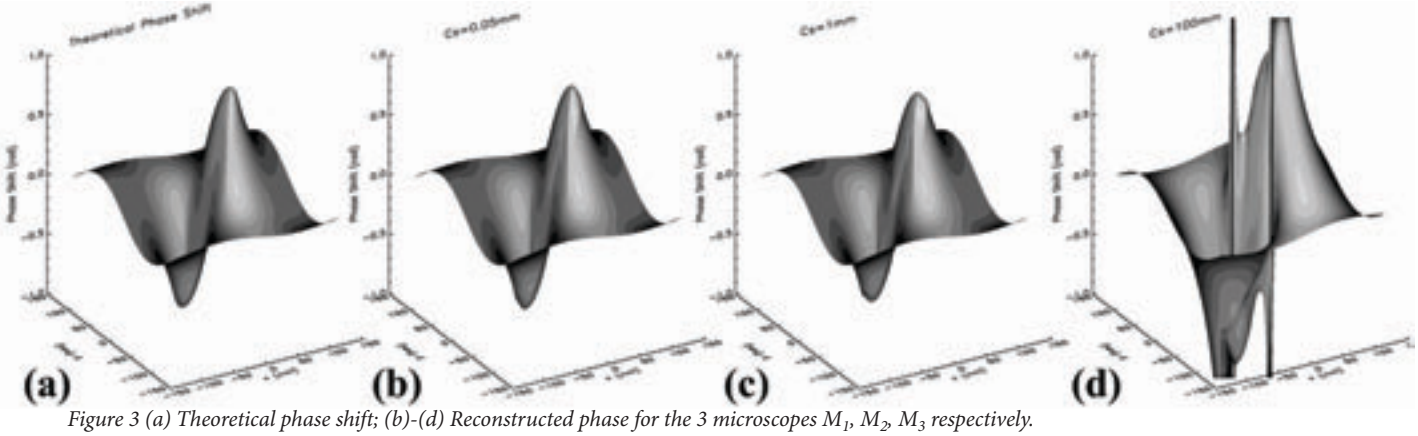


*Figure 3 (a) Theoretical phase shift; (b)-(d) Reconstructed phase for the 3 microscopes $M_1$, $M_2$, $M_3$ respectively.*

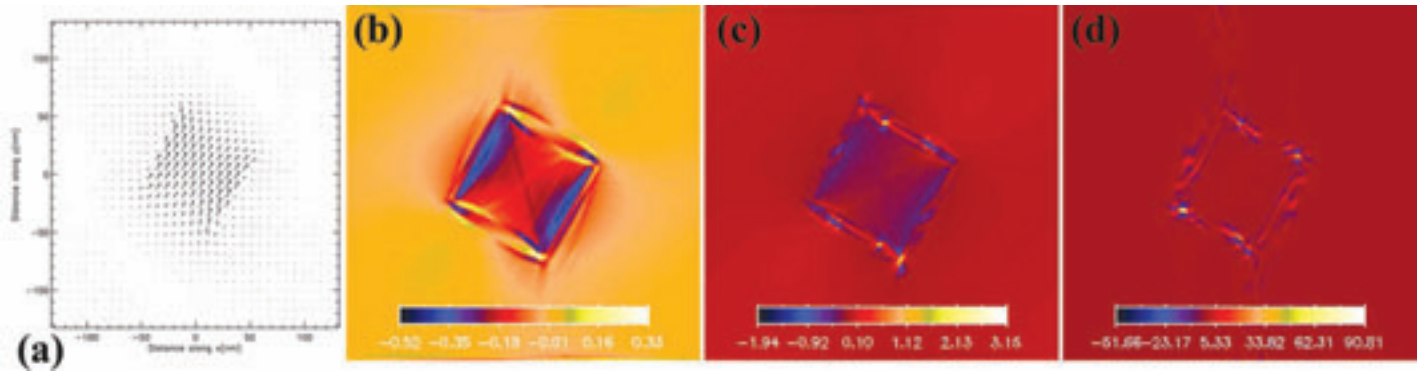


*Figure 4 (a) Theoretical field plot in the x-y plane and (b-d) shows the difference in reconstructed $B_x$ in the **x-y** plane and theoretical $B_x$ for microscopes $M_1$, $M_2$, $M_3$ respectively.*

**Table 1 Operational parameters for 3 different microscopes used for image simulations. The bottom row shows the root-mean-square error in the recovered phase.**

| Parameter | $M_1$ | $M_2$ | $M_3$ |
|---|---|---|---|
| $C_s$ (mm) | 0.05 | 1.0 | 100.0 |
| $q_c$ (mrad) | 0.2 | 0.6 | 0.6 |
| D (nm) | 3.0 | 8.8 | 8.8 |
| Df (nm) | 200 | 200 | 200 |
| RMSE | 0.0049 | 0.0085 | 0.1117 |

Figure 4(a) shows the theoretical induction in the center (*x-y*) plane of the particle; (b) – (d) show the difference between the x-component of the reconstructed field and the original field for each of the microscopes $M_1$, $M_2$ and $M_3$ respectively. Since the reconstruction of ***B*** relies on the recovered magnetic phase shift, it is important that the error in the phase shift recovery be minimized. It is clearly seen from Figure 3(b-d) that $C_s$ plays an important role in the phase shift recovery. Thus, for quantitative characterization of the 3D magnetic induction at the nano-scale, there is a need to use $C_s$ correctors in Lorentz mode. ■

## References

[1] Y. Aharonov and D. Bohm, *Phys. Rev*, 115 (1959) 485.
[2] D. Paganin and K.A. Nugent, *Phys. Rev. Letters*., 80, (1998) 2586.
[3] D.J. Rosier et al., *Nature*, 217 (1968) 130.
[4] G. Sparr and K.Strahlen, Tech. Rep., http://citeseer.ist.psu.edu/sparr98vector.html(1998).
[5] M. Beleggia et al., *Phil. Mag*., 83 (2003) 1143.
[6] This work was supported by the U.S Department of Energy, Basic Energy Sciences under contract number DE-FG02-01ER45893.